Simulation of trajectories of charged particles from solar winds in Earth's magnetic field

Kasper Eikeland

Department of Physics, Norwegian University of Science and Technology
Dated 17.03.2024

1 Introduction

The charged particles originating from solar winds excite the gas in the upper atmosphere of the Earth, which in turn gives rise to the auroras seen in the nightsky of the Northern hemisphere (Chen 2015). In this study we seek to better understand the motion and trajectories of these charged particles subject to the Lorentz force from the magnetic field of the Earth.

To simulate the trajectories of these charged particles, the magnetic field of the Earth is modelled as a dipole field. This model is only sufficiently accurate for distances less than $6R_E$ (Soni et al. 2021) from the center of the Earth, where $R_E \approx 6380$km is the radius of the Earth. A more accurate model would be the model of (Hones Jr. 1963). For the sake of simplicity we compute the trajectories in the dipole model, even for initial positions of magnitude $> 6R_E$. This is to simulate the particles travelling from the Sun to the Earth. The magnetic north pole is tilted around 11° away from the rotational axis of the Earth, which itself is tilted at about 23° from the Earth-Sun ecliptic.

According to (Soni et al. 2021) the problem of computing the trajectories for solar wind particles requires higher numerical precision than that of RK4. This is because of numerical instabilities which arise for the trajectories of lower energy protons and electrons. Still, the authors argue that the charged particles from solar winds are accelerated to ∼MeV speeds, which make them suitable for simulation using fourth order Runge-Kutta methods. For this study we compute the trajectories of protons with a kinetic energy between 100eV and 1MeV using RK45. The resulting trajectories are validated by considering the conservation of the kinetic energy.

2 Theory

As a magnetic dipole field, the magnetic field of the Earth is given in coordinate-free form (Griffiths 2024) as

$$\boldsymbol{B}(\boldsymbol{r}) = \frac{\mu_0}{4\pi r^3}[3(\boldsymbol{M}\cdot\hat{\boldsymbol{r}})\hat{\boldsymbol{r}} - \boldsymbol{M}], \tag{1}$$

where $\boldsymbol{M}$ is the magnetic dipole moment of the Earth, μ_0 is the vacuum permeability and $\boldsymbol{r} = (x, y, z)$ is the position vector. Equation (1) can be written in cartesian coordinates as

$$\boldsymbol{B}(\boldsymbol{r}) = \frac{\mu_0}{4\pi r^5}\begin{bmatrix} 3x^2 + r^2 & 3xy & 3xz \\ 3xy & 3y^2 + r^2 & 3yz \\ 3xz & 3yz & 3z^2 - r^2 \end{bmatrix}\boldsymbol{M}. \tag{2}$$

At the magnetic equator ($\boldsymbol{r} \perp \boldsymbol{M}$), the magnetic field strength is measured to $B_0 \approx 3.07 \times 10^{-5}$T (Soni et al. 2021). Therefore, the magnitude of the Earths magnetic dipole moment is given by (2) as

$$M = \frac{4\pi}{\mu_0} R_E^3 B_0, \tag{3}$$

where R_E is the radius of the Earth. In this simulation the Earth is placed at the origin of the coordinate system, and the x-axis is along the Sun-Earth axis. The magnetic dipole moment $\boldsymbol{M}$ is rotated $11° + 23°$ around the y-axis.

The relativistic equation of motion for a charged particle of charge q and mass m moving in a magnetic field is given by the Lorentz force

$$\gamma m \frac{\mathrm{d}\boldsymbol{v}}{\mathrm{d}t} = q\boldsymbol{v} \times \boldsymbol{B}(\boldsymbol{r}), \tag{4}$$

where $\boldsymbol{v}$ is the velocity vector of the particle, and γ is the Lorentz factor given as

$$\gamma = \frac{1}{\sqrt{1 - v^2/c^2}}, \tag{5}$$

where c is the speed of light. For a particle moving only in a magnetic field, γ is constant, as it only depends on the squared magnitude of the velocity, which is unchanged by the Lorentz force (Griffiths 2024). The magnitude of the velocity of the particle is obtained from the kinetic energy K of the paricle as

$$v = c\sqrt{1 - \left(\frac{mc^2}{mc^2 + K}\right)^2}. \tag{6}$$

The position of the particle can be found by integrating the position-velocity relation

$$\frac{\mathrm{d}\boldsymbol{r}}{\mathrm{d}t} = \boldsymbol{v}. \tag{7}$$

Equations (4) and (7) are solved using RK45 (Dormand and Prince 1980).

In a uniform magnetic field, the charged particles will gyrate around the magnetic field lines with the gyro-frequency

$$\omega_g = \frac{q|\boldsymbol{B}|}{\gamma m}, \tag{8}$$

stemming from the cross product in (4). The gyro-radius is given (Chen 2015) by

$$r_g = \frac{mv_\perp}{q|\boldsymbol{B}|}, \tag{9}$$

where $v_\perp$ is the component of $\boldsymbol{v}$ perpendicular to $\boldsymbol{B}$. The dipole field (2) however, is non-uniform with a non-zero gradient $\nabla|\boldsymbol{B}|$. This gradient and curvature of the field introduces two additional forms of motion: an azimuthal drift around the axis of the magnetic dipole, and a periodic bouncing motion along the magnetic field lines (Chen 2015).

If $\nabla|\boldsymbol{B}| \neq 0$ the gyro-radius (9) changes. In regions of higher field strength r_g decreases. Similarly, r_g increases in regions of higher field strength. This causes a drift motion perpendicular to $\nabla|\boldsymbol{B}|$.

Due to the component of $\boldsymbol{v}$ parallell to $\boldsymbol{B}$ in (4), the particles move along the magnetic field lines. As the gradient $\nabla\boldsymbol{B}$ is parallell to $\boldsymbol{B}$ for the dipole field, there will be magnetic mirrors present (Chen 2015). These magnetic mirrors trap the charged particles by reflecting the velocity parallell to the field lines. Thus the particle oscillates between the magnetic mirrors along the magnetic field lines.

3 Methods

For this analysis, different trajectories are computed for different initial conditions. The simulations are run for protons of kinetic energy between 100eV and 1MeV. The initial velocities of the protons is then given by $\boldsymbol{v_0} = (v, 0, 0)$ where v is given by equation (6) with $m = m_p \approx 1.67 \times 10^{-27}$kg being the mass of the proton. The initial positions of the protons are given as

$$\begin{aligned} x_0 &\in [-2R_E, -12R_E], \\ y_0 &\in [-R_E, R_E], \\ z_0 &\in [-R_E, R_E]. \end{aligned}$$

The values for x_0, y_0, z_0 are sampled evenly in the given intervals with a sample size of $n_x = 11$, n_y, $n_z = 3$. Thus, for each level of kinetic energy, $n_x \cdot n_y \cdot n_z = 99$ trajectories are computed. All protons are simulated as particles travelling from the Sun to the Earth, i.e. $x_0 < 0$ and $v_y, v_z = 0$. All trajectories are computed for a timespan of 120s.

The simulation code is written in the Python programming language. The equations of motion (4) and (7) are solved using RK45 as implemented in the Python library SciPy (SciPy 2024). Consult the supplementary material (Eikeland 2024) for further details.

4 Results

Two-dimensional plots of the magnetic field lines are shown in figure 1 for both the xz-plane at $y = 0$ and the xy-plane at $z = -2R_E$. Observe that the magnetic poles are tilted away from the z-axis.

Figure 2 (a-h) shows the projection onto the xy- and xz-plane of 4 different trajectories computed for different initial conditions. The red circle indicates the Earth. In all cases, the less energetic protons cover less distance in the same time span as the more energetic protons. The trajectories given in figures 2 (a-c) and (e-g) display drift motion of the protons around the axis of the magnetic dipole. Furthermore, the trajectories display both bouncing along the field lines and gyration around the field lines. The gyro-frequency increases as the protons approach the mirror points, as depicted in figures 2b, 2c, 2f and 2g. Figures 2a and 2e display a higher frequency for the drift motion than that of figures 2b, 2c, 2f and 2g. The bouncing frequency of figure 2b and 2f is evidently higher than that of figures 2c and 2g. Figures 2d and 2h show the trajectory of a proton starting far away from the Earth. In this case, the proton escapes the magnetic field of the Earth. The motion displayed in figures 2a and 2e is still confined to the Earth's magnetoshpere.

To validate the computed trajectories we use the fact that the kinetic energy is conserved for a charged particle only subject to an external magnetic field (Griffiths 2024). Figure 3 shows the deviation of the kinetic energy for 5 different simulations of protons at 100eV, 10keV and 1MeV as a function of time.

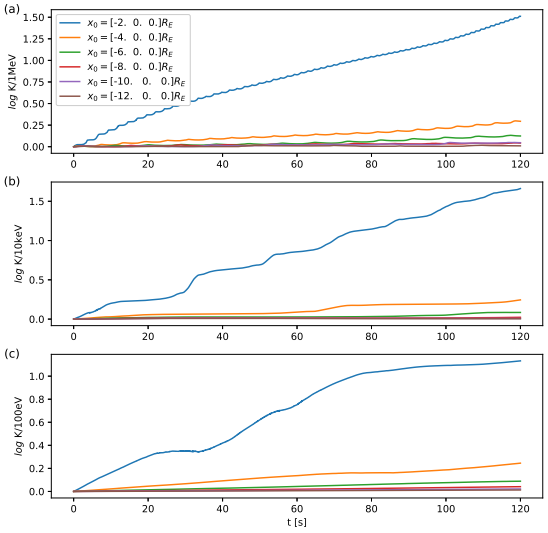

Figure 3: The deviation of the kinetic energy of the simulated particles as a function of time for different initial conditions. (a): 1MeV protons, (b): 10keV protons, (c): 100eV protons.

The plots indicate that the kinetic energy grows with time for the protons with initial position close to the Earth.

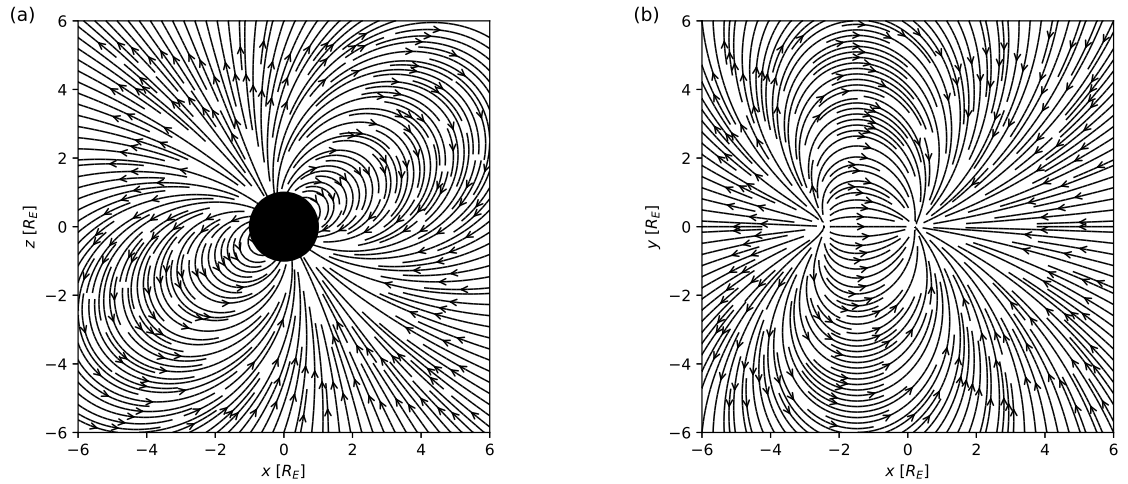

Figure 1: Streamline plots of the magnetic field lines computed via equation (2). (a): The magnetic field lines in the xz-plane at $y = 0$. The black circle indicates the Earths. (b): The magnetic field lines in the xy-plane at $z = -1R_E$. The magnetic equator is tilted around the y-axis towards the sun, i.e in the negative x-direction

5 Discussion

The trajectories shown in figure 2 display both gyration and azimuthal drift, as well as confinement due to the magnetic mirrors present in the dipole field. For figures 2d and 2h however, the proton is not confined to the magnetoshpere. (Chen 2015) argues that a particle with small $v_\perp/v_{||}$ will escape if the magnetic field is not strong enough. This may be the case as the magnetic field is weaker farther away from the Earth. One can also argue that it is not the case, as the trajectories in figures 2c and 2g are confined, and are almost as far away from the Earth. Due to time constraints this issue was not further investigated, and it is left as an open question.

Interpreting the trajectories as the motions of charged particles from solar winds may be faulty in this dipole model. Specifically, the infalling of charged particles towards the north and south magnetic poles is not observed. Still it is known that this is the cause of the auroras which have readily been observed (Chen 2015). This may be due to the discrepancy between our dipole model and the real magnetic field of the Earth. The static orientation of the magnetic field wrt. the Sun may be a cause. In our model, the magnetic dipole is tilted away from the Sun. The orientation of the magnetic field precesses with the Earth's axis of rotation as well as moving on its own (Barker and Barraclough 1980). This is not taken into account in this model. Furthermore, as mentioned in the introduction, the dipole model is only a reasonable apporximation for $|\boldsymbol{r}| < 6R_E$. Our simulations thus suggest that the particles that reach the inner magnetosphere ($|\boldsymbol{r}| < R_E$) sufficiently close to the magnetic equator are confined to orbital motion around the Earth. They drift azimuthally and bounce between the magnetic mirrors, never reaching the north or south magnetic poles. This is in accordance with the results of (Soni et al. 2021). To fully grasp the trajectories of charged particles from solar winds then, one may need a more sophisticated model of the Earth's magnetic field.

The results from considering the conservation of kinetic energy show that the kinetic energy grows with time when the protons are close to the Earth. This indicates that there is a need for a higher precision numerical scheme for this case. Moreover, the results show no significant sign of increased numerical instability for protons with lower energy as mentioned for RK4 in (Soni et al. 2021). This may be due to the higher precision of RK45, as implemented in SciPy, compared to the ordinary RK4 method (Dormand and Prince 1980). Thus it seems reasonable to apply RK45 for the task of simulating the trajectories of charged protons in Earth's inner magnetoshpere for $|\boldsymbol{r}| \in (4R_E, 6R_E)$. For $|\boldsymbol{r}| < 4R_E$ a higher precision numerical scheme may be needed. The results of (Soni et al. 2021) suggest that RK6 suffices.

6 Conclusion

The magnetic field of the Earth was modeled as a magnetic dipole tilted about the y-axis. The trajectories of protons with energies of 100eV, 10keV and 1MeV were calculated via the Lorentz force (4) using RK45. The trajectories were computed for 99 different initial conditions. Most of the trajectories display gyration, azimuthal drift and bouncing motions. This

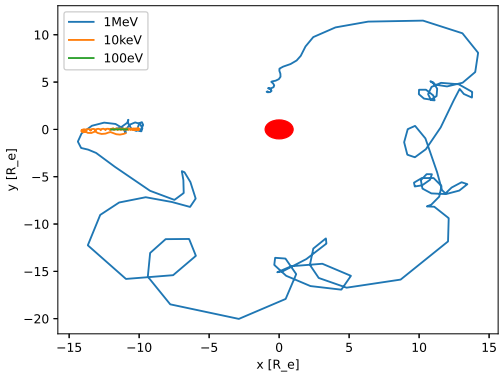

(a) $x_0 = [-12.0, 0.0, -1.0]R_E$, xy-plane.

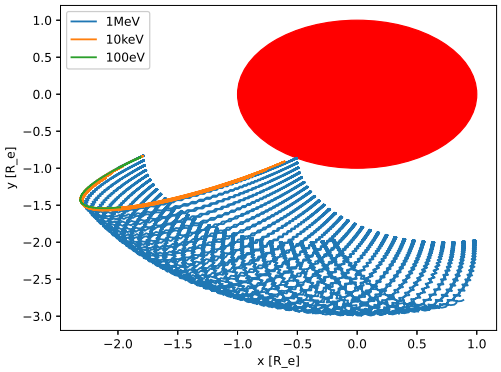

(b) $x_0 = [-2.0, -1.0, 0.0]R_E$, xy-plane.

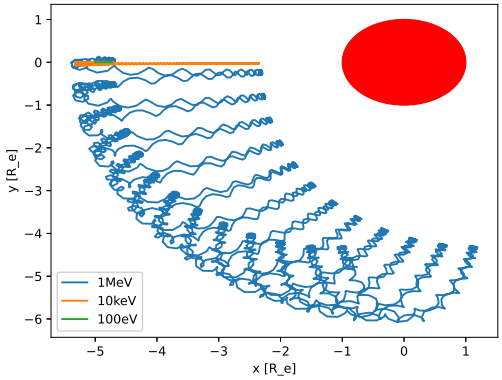

(c) $x_0 = [-5.0, 0.0, -1.0]R_E$, xy-plane.

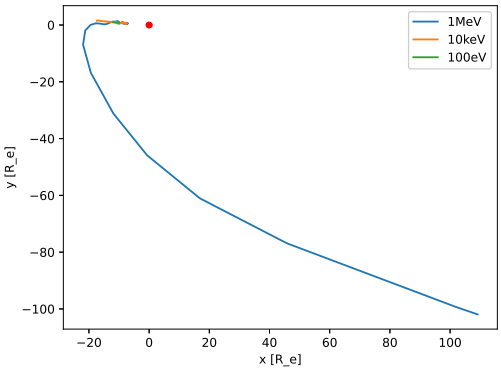

(d) $x_0 = [-12.0, 1.0, 1.0]R_E$, xy-plane.

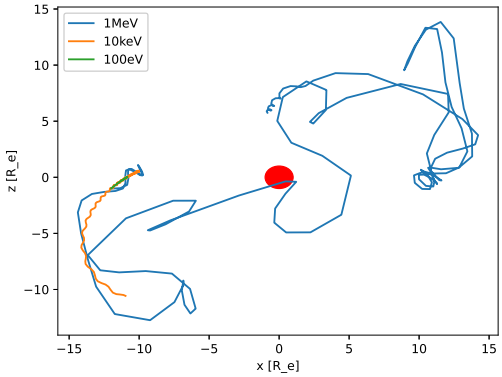

(e) $x_0 = [-12.0, 0.0, -1.0]R_E$, xz-plane.

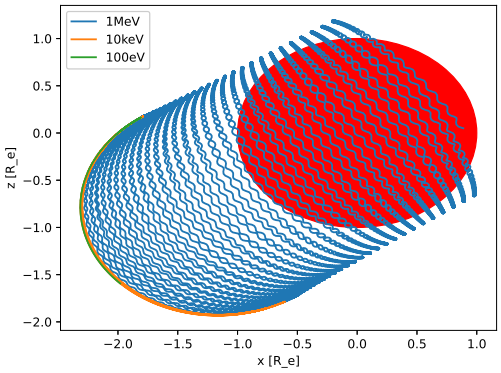

(f) $x_0 = [-2.0, -1.0, 0.0]R_E$, xz-plane.

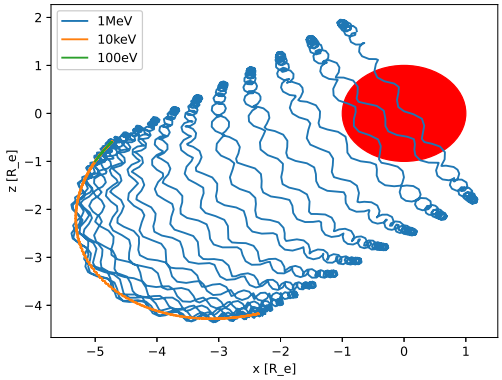

(g) $x_0 = [-5.0, 0.0, -1.0]R_E$, xz-plane.

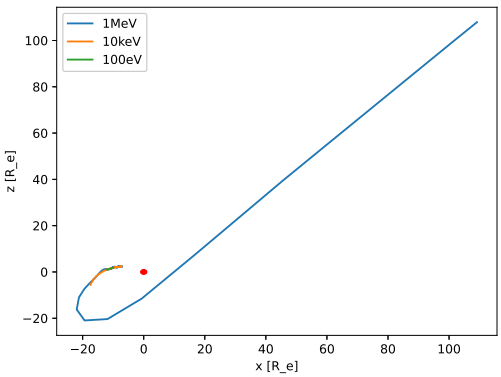

(h) $x_0 = [-12.0, 1.0, 1.0]R_E$, xz-plane.

Figure 2: Trajectories of 100eV, 10keV and 1MeV protons projected onto the xy- and xz-planes. The initial positions of the protons are noted in the subcaptions. The trajectories are selected from the aforementioned 99 simulations for each energy level. They are chosen as a representative subset to demonstrate the different motions. See supplementary material (Eikeland 2024) for a complete set of calculated trajectories.

motion is confined to the Earth's magnetosphere for most initial conditions. For some particular inital conditions the motion is not confined. No motion towards the north or south magnetic poles were observed. To model the trajectories of charged particles from solar winds as the source of the auroras, one may need a more realistic model of the Earth's magnetic field. The simulations suggest that the motion of protons within Earth's magnetosphere is confined to orbital motion around the Earth, in accordance with (Soni et al. 2021). Finally, the results suggest that RK45 is sufficient for simulating motion with $|\boldsymbol{r}| \in (4R_E, 6R_E)$. For $|\boldsymbol{r}| < 4R_E$ a more precise numerical scheme may be needed.

References

Barker, F. S. and D. R. Barraclough (1980). 'World magnetic chart model for 1980'. In: *EOS Transactions* 61.19, pp. 452–453. DOI: 10.1029/EO061i019p00452-04.

Chen, Francis F. (2015). *Introduction to Plasma Physics and Controlled Fusion*. Springer Cham.

Dormand, J.R. and P.J. Prince (1980). 'A family of embedded Runge-Kutta formulae'. In: *Journal of Computational and Applied Mathematics* 6.1, pp. 19–26. ISSN: 0377-0427. DOI: https://doi.org/10.1016/0771-050X(80)90013-3. URL: https://www.sciencedirect.com/science/article/pii/0771050X80900133.

Eikeland, Kasper (2024). *Supplementary material*. URL: https://github.com/kreikeland/tfy-4220-project.

Griffiths, David J. (2024). *Introduction to Electrodynamics*. 5th ed. Cambridge University Press.

Hones Jr., Edward W. (1963). 'Motions of charged particles trapped in the Earth's magnetosphere'. In: *Journal of Geophysical Research (1896-1977)* 68.5, pp. 1209–1219. DOI: https://doi.org/10.1029/JZ068i005p01209. URL: https://agupubs.onlinelibrary.wiley.com/doi/abs/10.1029/JZ068i005p01209.

SciPy (2024). *scipy.integrate.solve_ivp - SciPy v1.12.0 Manual*. Retrieved 15.03.2024 from https://docs.scipy.org/doc/scipy/reference/generated/scipy.integrate.solve_ivp.html.

Soni, Pankaj K., Bharati Kakad and Amar Kakad (2021). 'Simulation study of motion of charged particles trapped in Earth's magnetosphere'. In: *Advances in Space Research* 67.2, pp. 749–761. ISSN: 0273-1177. DOI: https://doi.org/10.1016/j.asr.2020.10.020. URL: https://www.sciencedirect.com/science/article/pii/S0273117720307481.